Reversible Clustering of pH- and Temperature-Responsive Janus Magnetic Nanoparticles

Tatsushi Isojima,[†] Marco Lattuada,[‡] John B. Vander Sande,[§] and T. Alan Hatton[†,*]

[†]Department of Chemical Engineering, and [§]Department of Materials Science and Engineering, Massachusetts Institute of Technology, 77 Massachusetts Avenue, Cambridge, Massachusetts 02139, and [‡]Institute for Chemical and Bioengineering, HCI F135, ETH Zurich, Wolfgang-Pauli Strasse 10, 8093 Zurich, Switzerland

ABSTRACT Janus nanoparticles have been synthesized consisting of ~5 nm magnetite nanoparticles coated on one side with a pH-dependent and temperature-independent polymer (poly(acrylic acid), PAA), and functionalized on the other side by a second (tail) polymer that is either a pH-independent polymer (polystyrene sodium sulfonate, PSSNa) or a temperature-dependent polymer (poly(*N*-isopropyl acrylamide), PNIPAM). These Janus nanoparticles are dispersed stably as individual particles at high pH values and low temperatures, but can self-assemble at low pH values (PSSNa) or at high temperatures (>31 °C) (PNIPAM) to form stable dispersions of clusters of approximately 80−100 nm in hydrodynamic diameter. The Janus nanoparticle compositions were verified using FTIR and XPS, and their structures observed directly by TEM. Their clustering behavior is analyzed by dynamic light scattering and zeta potential measurements.

KEYWORDS: functional nanoparticle · Janus nanoparticle · magnetite (Fe_3O_4) · self-assembly

There has been increasing interest in recent years in the potential applications of functionalized nanoparticles, with a concomitant strong scientific focus on their fundamental properties. These functional entities, prominent among which are magnetic, metal, and metal oxide nanoparticles, are applied in a wide range of fields, including drug delivery systems, diagnostics, gene analysis, proteomics, affinity purifications, quantum dots, and the like. In particular, magnetic nanoparticles have been investigated for many applications such as environmental and biomolecular separations, magnetic resonance imaging (MRI), magnetic drug targeting and delivery, and hyperthermia technology for cancer treatment. There are undoubtedly still many gains to be made in the synthesis, functionalization, characterization, and applications of these systems.

The current trend in research on nanoparticles is focused on controlling their size and shape to ensure narrow distributions,[1,2] on developing hybrid materials with metals or metal oxides,[3−5] and on functionalizing the particles with soft materials.[6−9] The directed clustering of nanoparticles is a promising research tool for the development of new materials with a wide range of potential applications,[10−13] especially when such clustering can be controlled by application of an appropriate stimulus such as pH, temperature, chemical addition, or light, for example.[6,7,11,13] Cluster size and shape cannot be controlled using symmetrically functional core−shell nanoparticles as they tend to aggregate uncontrollably and precipitate out of suspension. Janus nanoparticles, on the other hand, have asymmetric surface properties and show promise for the control of self-assembled nanoparticle cluster sizes. Much of the research on Janus particles has been on the preparation of particles on the order of hundreds of nanometers to a few micrometers,[14] that is, submicrometer particles rather than true nanoparticles.

Janus *nano*particles have been reported recently by a few researchers. For example, Chen *et. al* prepared gold Janus nanoparticles by trapping the nanoparticles within a Langmuir monolayer and then performing a ligand exchange reaction with the surface moieties that were exposed to the bulk liquid solution.[15,16] Gu *et. al* created Janus nanoparticles similarly by immobilizing nanoparticles at the surfaces of emulsion droplets.[17] The kinds of nanoparticles formed under these conditions are inherently and permanently amphiphilic, and so will self-assemble automatically; stable single nanoparticle dispersions are unlikely to be attainable, and external control of their clustering behavior may be difficult.

We have recently developed an approach for the synthesis of stimuli-responsive Janus

*Address correspondence to tahatton@mit.edu.

Received for review February 12, 2008 and accepted August 07, 2008.

Published online September 3, 2008.
10.1021/nn800089z CCC: $40.75

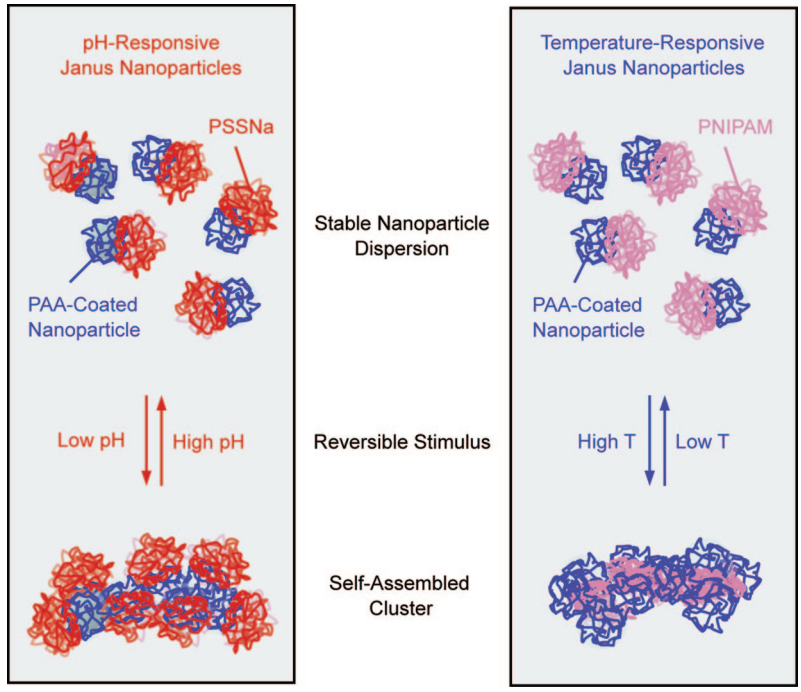

Figure 1. Schematic representation of the Janus nanoparticles and their self-assembled structures on application of an appropriate stimulus. Note that the PSSNa polymers constitute the stabilizing shell of the clusters, while the PNIPAM chains collapse and form the hydrophobic core of the clusters.

nanoparticles having both faces composed of hydrophilic materials, but with different polymer chemical characteristics, at least one of them exhibiting a definite response to an applied stimulus, in this case pH.[18] The reversible self-assembly of these ~11 nm nanoparticles on lowering or raising the pH of the solution was demonstrated and reconciled with the results of a Monte Carlo simulation. The structure of the Janus nanoparticles was inferred from their observed clustering behavior, but no direct evidence of this structure was given. The purpose of this paper is to show that Janus nanoparticles can be prepared readily using even smaller magnetite nanoparticles (5 nm) coated with a pH-dependent and temperature-independent polymer (poly(acrylic acid), PAA), which are functionalized on one side only by a second polymer that is either a pH-independent anionic polymer (polystyrene sulfonate, PSSNa) or a temperature-dependent nonionic polymer (poly(*N*-isopropyl acrylamide), PNIPAM) having a well-defined lower critical solution temperature (LCST).[19] The self-assembly properties of these two classes of Janus nanoparticles in response to appropriate stimuli are also reported. Finally, we provide, for the first time, direct evidence for the asymmetric attachment of the second polymer to the nanoparticles.

RESULTS AND DISCUSSION

Design of Stimulus-Responsive Janus Nanoparticles. A primary goal of this work was the synthesis of stimuli-responsive Janus nanoparticles that can be induced to form micelle-like self-assembled structures through the application of an appropriate stimulus and that can be redispersed to again give stable, singly dispersed nanoparticles on removal of this stimulus. The Janus structures synthesized in this work consisted of 5 nm magnetite nanoparticles, each coated uniformly with a PAA shell that was functionalized further by the asymmetric attachment of a second polymer to one side of the surface coating as shown in Figure 1. The second polymer used was either pH-independent PSSNa or temperature-dependent PNIPAM.

PAA was selected as the base coating because its numerous carboxyl groups provide (i) strong anchoring of the polymer shell to the nanoparticles through chelation with the iron atoms on the particle surface, (ii) ready attachment of functional groups using, for example, amidation chemistry, and (iii) pH-responsive behavior since it is fully charged well above its pK_a of 4.5, and uncharged well below this pH value, with intermediate charge states at pH values within one pH unit on either side of the pK_a. When charged, the PAA-coated nanoparticle suspensions are stabilized by electrostatic repulsions between the particles, while at low pH the particles aggregate and precipitate from suspension.

We prepared two types of Janus nanoparticles. The first was a pH-responsive particle, where the attached polymer was strongly charged and independent of pH, but the exposed PAA portion was hydrophilic (charged) or hydrophobic (uncharged) depending on the pH. Thus at low pH values, this nanoparticle was amphiphilic allowing for micelle-like self-assembly to form finite-sized clusters, but at higher pH values the entire nanoparticle was charged and could not aggregate with other nanoparticles. The second Janus nanoparticle consisted of a hydrophilic, charged PAA shell (at high pH) to which was attached the widely studied thermally sensitive polymer, PNIPAM, which has a lower critical solution temperature (LCST) of ~30 °C in water.[19] Above the LCST, PNIPAM is dehydrated and the collapsed polymer is hydrophobic, so that at these higher temperatures the Janus nanoparticles become amphiphilic, and begin to self-assemble to form finite clusters stabilized by the exposed, charged PAA shell.

Preparation of PAA-Coated Magnetic Nanoparticles. Monodispersed 5 nm magnetic nanoparticles stabilized in an organic solvent by mixed oleyl acid/oleyl amine (OA/OAm) surface monolayers were synthesized by the method of Sun *et al.*[1,2] The nonreactive OA/OAm coating was replaced by galactaric acid *via* a ligand exchange reaction; the galactaric acid was then esterified with 2-bromoisobutyryl bromide to form Br-terminated

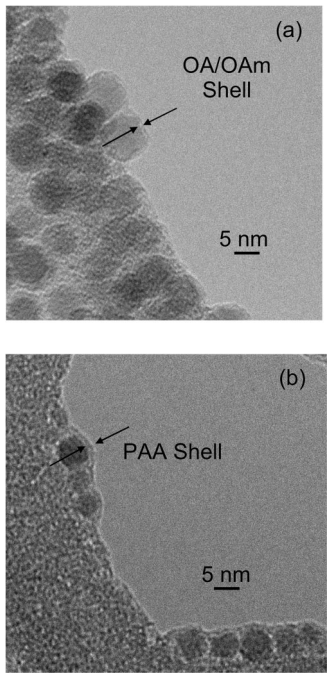

Figure 2. TEM images of (a) OA/OAm monolayer coated magnetic nanoparticles and (b) PAA-coated core−shell magnetic nanoparticles.

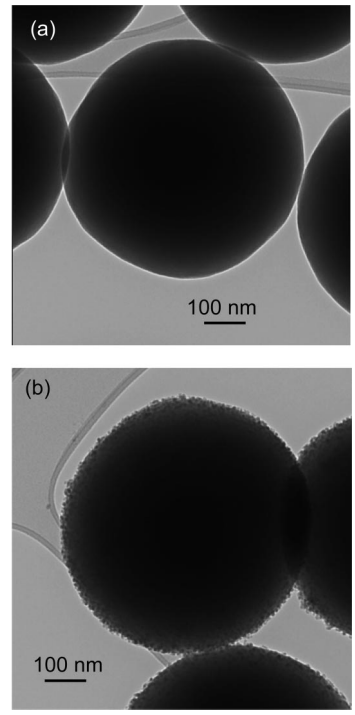

Figure 3. TEM images of (a) a bare silica bead and (b) a heteroparticle with silica beads covered by a monolayer of PAA-coated magnetic nanoparticles.

magnetic nanoparticle coatings that served as initiators in the synthesis of a poly-trimethylsilyl acrylate (poly-TMSA) coating by atom-transfer radical polymerization (ATRP).[6] Deprotection of the poly-TMSA polymer shell yielded the desired PAA-coated magnetic nanoparticles.

Figure 2a gives a TEM image of the magnetic nanoparticles as synthesized, coated with an OA/OAm monolayer, while the final PAA-coated nanoparticles are shown in Figure 2b. Since the contrast between the coatings (either the OA/OAm monolayers or the PAA polymer shells) and the carbon film of the grid for the TEM is poor, we used lacey carbon grids, that is, thin carbon films perforated with holes, to probe the structures of the coated nanoparticles; particles which protrude into the holes in the carbon film do not suffer from this overlapping problem, and the shell coatings can be visualized more clearly. The thin OA/OAm monolayer surrounding the particles is evident in Figure 2a, as is the thicker PAA shell of the final particles in Figure 2b.

The molecular weight and polydispersity of the polymer coating were determined by removing the poly-TMSA coatings on the intermediate magnetic nanoparticles with iodine (5 M) and subjecting the released polymer to gel permeation chromatography (GPC) analysis. The number and weight averaged molecular weights were found to be 4660 and 5160, respectively, giving a polydispersity index (PDI) of 1.11, which is consistent with that expected from living polymerization (PDI < 1.5).[20] Thermogravimetric analysis (TGA) of the coated nanoparticles indicated that the OA/OAm and PAA shells contributed 17 and 45 wt %, respectively, to the total mass of the particles. The value for the OA/OAm shell suggests a collapsed surfactant monolayer thickness of about 0.5−1 nm, and that for the PAA shell a thickness of about 1.5 nm. These values are in line with the TEM observations.

Preparation of Janus Nanoparticles. The Janus nanoparticles were prepared by first masking one face of the negatively charged PAA-coated nanoparticles by immobilization of these particles on the surfaces of functionalized, positively charged 600 nm silica beads, and then covalently attaching the desired second polymer to the exposed faces of the nanoparticles.

The silica beads were synthesized by the Stöber method[21,22] and rendered positively charged through silylation by *N*-trimethoxysilylpropyl-*N*,*N*,*N*-trimethylammonium chloride (TMSPTMAC). This latter step changed the zeta (ζ) potential of the silica beads from −52 to +60 mV. The positively charged bare silica beads were dispersed in a suspension of PAA-functionalized magnetic nanoparticles at a pH of 6, resulting in their being coated with a monolayer of these nanoparticles through electrostatic adsorption; the reversal of sign of the ζ potential on the beads, which changed to −40 mV, indicated a successful coating of the beads. Figure 3a shows a TEM image of a bare silica bead, while Figure 3b shows uniform monolayer coverage of the bead with the PAA-coated nanoparticles.

The surfaces of the nanoparticles facing the silica beads were protected from further functionalization, but the exposed surfaces of the nanoparticles could be functionalized through the attachment of amino-end

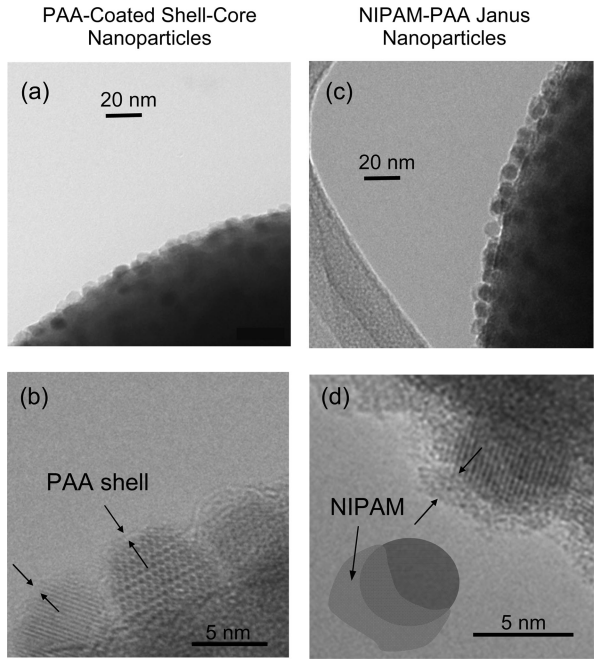

Figure 4. HRTEM images of the magnified area near the surface of (a, b) a hetero particle consisting of a silica bead covered with PAA-coated magnetite nanoparticles, and (c, d) these adsorbed nanoparticles after functionalization with the second polymer, PNIPAM to give Janus−PNIPAM nanoparticles. Figure 4d contains a cartoon to aid the reader in interpreting the polymer tail structure.

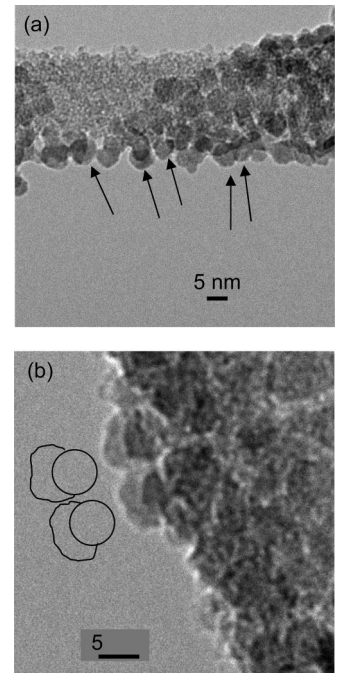

Figure 5. TEM images of Janus−PSSNa magnetic nanoparticles. These images were taken at a defocus condition (see the bright Fresnel fringe at the particle perimeters) to enhance contrast. (a) The arrows indicate the Janus nanoparticles with exposed tails protruding into the holes of the lacey carbon grid

functionalized polymers, either PSSNa or PNIPAM, through amidation chemistry. The TEM images in Figure 4a,b show the adsorbed PAA-coated core−shell nanoparticles on the silica bead surface, while those in Figure 4c,d give high resolution images of the adsorbed nanoparticles after the attachment of PNIPAM as the second polymer, in which the nanoparticle crystals and the amorphous attached polymers can be discerned more readily. Also indicated on these figures are arrows showing the different polymer layers to emphasize clearly the structures that are formed; these figures confirm the successful attachment of the second polymer on the exposed surfaces of the PAA-coated magnetic nanoparticles.

The Janus particles were recovered by increasing the pH of the solution to ~12 to induce a charge reversal on the silica bead surfaces and thereby to repel the adsorbed nanoparticles. Figure 5 shows TEM images of the PSSNa-Janus particles following detachment from the silica surface. Owing to the effective contrast between Fe_3O_4 and PSSNa, we can clearly identify the anisotropic structures of the Janus nanoparticles, which have been emphasized by the line tracings of these structures. Note that the Janus properties are not evident for all particles as the nanoparticles will be somewhat randomly oriented around the edges of the lacey carbon so that sometimes the attached polymer will be hidden from view, or will be in regions where the contrast is not sufficient to be able to identify them.

Analysis of Janus Particles. Further evidence for the attachment of either PSSNa or NIPAM to the PAA-coated magnetic nanoparticles was furnished by Fourier transform infrared (FTIR) spectroscopy and X-ray photoelectron spectroscopy (XPS).

The FTIR spectrum of PSSNa shown in Figure 6a has absorption bands at wavenumbers between 1100 and 1200 cm^{-1}, which are attributed to the $R-SO_2-O$ group;[23] PAA does not absorb in this region and thus the presence of these bands in the Janus−PSSNa nanoparticle spectrum in Figure 6a, confirms the successful attachment of the PSSNa to the PAA-coated core−shell nanoparticles.

NIPAM has absorption bands at wavenumbers of 1670 and 1580 cm^{-1} corresponding to amide I and amide II, respectively, as shown in Figure 6b, while the PAA-coated magnetic nanoparticles have absorption bands at wavenumbers between 1800 and 1400 cm^{-1} that are attributed to the presence of COOH and coordinated $-COO^-$ groups.[24] There is some indication of the amide bands at 1670 and 1580 cm^{-1} in the Janus−PNIPAM nanoparticle spectrum, intimating that the PNIPAM attachment to the PAA-coated nanoparticles was successful.

The presence of the second polymer (PSSNa or PNIPAM) on the Janus nanoparticles was also confirmed by XPS. The detected elements were sulfur for PSSNa and nitrogen for PNIPAM. Neither of these elements was evident in the spectrum for the PAA-coated magnetic nanoparticles, but the peaks of S 2s (229 eV)

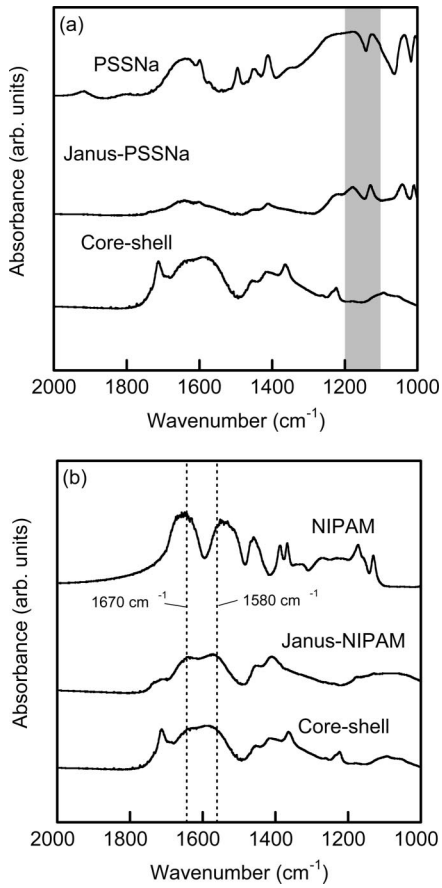

Figure 6. FTIR analysis of (a) Janus−PSSNa and PAA-coated core−shell magnetic nanoparticles, and pure PSSNa, and (b) Janus−PNIPAM and PAA-coated core−shell magnetic nanoparticles, and pure PNIPAM. The shaded region and dotted lines represent the amide and carboxyl groups for the PSSNa and PNIPAM polymers, respectively. Their absence in the PAA-coated nanoparticles, but presence in the Janus nanoparticles provides evidence for the attachment of the second polymers to the PAA-coated nanoparticles.

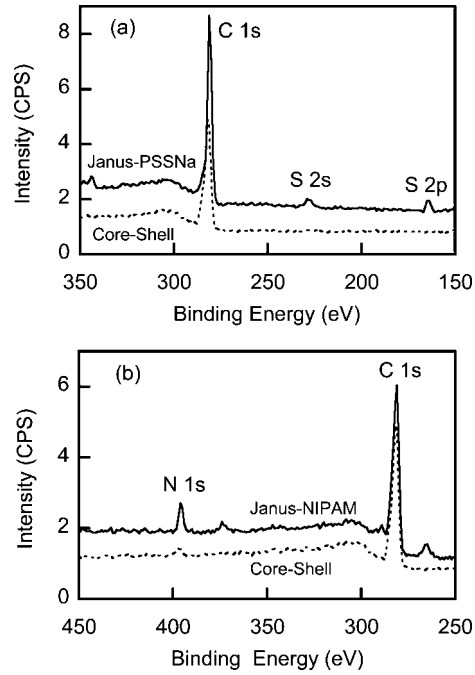

Figure 7. XPS spectra of (a) Janus−PSSNa and PAA-coated core−shell magnetic nanoparticles and (b) Janus−PNIPAM and PAA-coated core−shell magnetic nanoparticles.

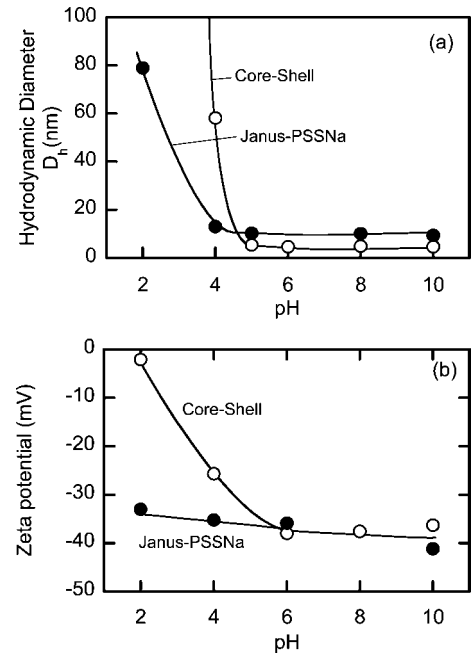

Figure 8. The pH dependent behavior of PAA-coated core−shell and Janus−PSSNa nanoparticles. (a) DLS measurements indicate uncontrolled growth of the PAA-coated nanparticles for pH > pK_a, while the Janus−nanoparticle aggregates are stabilized with hydrodynamic diameters of about 80 nm. (b) The ζ potential of the PAA-coated nanoparticles approaches zero at low pH, and thus the particle suspension is not stabilized by electrostatic interactions. The ζ potential of the Janus nanoparticles does not change appreciably because of the strong charge on the PSSNa group.

and S 2p (164 eV) for Janus−PSSNa nanoparticles in Figure 7a and N 1s (396 eV) for Janus−NIPAM nanoparticles in Figure 7b indicate the presence of these polymers. The atomic concentrations were found to be 3.2% for sulfur and 5.73% for nitrogen relative to carbon (C 1s, 281 eV) from which we estimated that the mass ratio of the second polymer to the PAA coating was about 1:2.6 for the Janus−PSSNa nanoparticles and 1:2.2 for the Janus−NIPAM nanoparticle.

Stimulus-Responsive Clustering of Janus Nanoparticles. The ability to control the self-assembly and clustering behavior of the Janus nanoparticles through application of appropriate stimuli was demonstrated with both the pH and temperature-responsive Janus nanoparticles by measuring their effective hydrodynamic diameters under different conditions using dynamic light scattering (DLS).

The pH dependent behavior of both the PAA-coated and Janus−PSSNa nanoparticles is reflected in the hydrodynamic diameters shown in Figure 8a, and ζ potentials given in Figure 8b. At high pH values, both the exposed PAA surfaces and the attached PSSNa of the Janus−PSSNa nanoparticles were electrically charged (*ca.* −40mV) and a stable dispersion of single particles

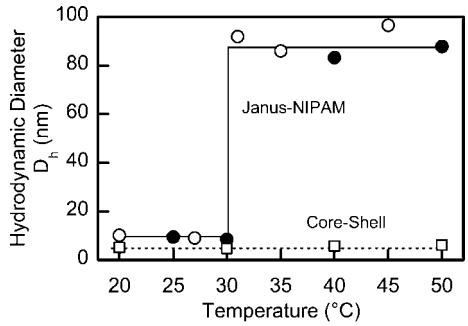

Figure 9. The effect of temperature on suspensions of PAA-coated core−shell and Janus−PNIPAM magnetic nanoparticles. The PAA-based suspensions are stable over the entire temperature range, but the PNIPAM-based nanoparticles form finite-sized clusters at temperatures above the LCST of NIPAM.

of approximately 10 nm was obtained. The PAA magnetic nanoparticles were also electrically charged (~−37 mV) and stably dispersed as single ~5 nm particles. The difference in hydrodynamic diameters between the core−shell and Janus nanoparticles is simply due to the presence of the attached polymer on the Janus particles. With reductions in pH to below the pK_a of PAA, the PAA-coated nanoparticles began to aggregate, and these aggregates grew without bound to precipitate out of suspension after some time. The Janus−PSSNa nanoparticles, on the other hand, also began to cluster, but their growth was limited by the strongly charged PSSNa groups, which, at pH 2, stabilized the clusters at a hydrodynamic diameter of about 80 nm. This self-assembly of the Janus PSSNa nanoparticles at pH 2 could be reversed readily by increasing the pH back to about 10 to obtain, once again, individually dispersed nanoparticles. This cycle could be repeated a number of times until the ionic strength increase due to the repeated additions of acid and base caused sufficiently high screening of the electrostatic repulsive interactions between the nanoparticles that the dispersions were no longer stable.

The temperature-dependent behavior of the Janus−NIPAM and PAA-coated magnetic nanoparticles measured by DLS is shown in Figure 9. While the PAA-coated nanoparticles were stable over the entire temperature range studied, this was not the case for the Janus nanoparticles, which were stably dispersed as individual nanoparticles with hydrodynamic diameters of ~10 nm at the lower temperatures only. At the phase transition temperature of PNIPAM (~31 °C), there was an abrupt increase in the average size of the dispersed entities with an average hydrodynamic diameter of ~90 nm, which was unchanged over the rest of the temperature range studied. The driving force for this self-assembly was the sudden change in the NIPAM properties from hydrophilic to hydrophobic at the LCST, while the charged PAA regions (−45 mV at 40 °C) inhibited unbridled growth of the clusters and stabilized them at a specific size. This self-assembly could be reversed by reducing the temperature to a value below the LCST. In Figure 9, the filled circles denote the response when the suspension was heated to that temperature, while the hollow circle symbols indicate the behavior on cooling to that condition from a higher temperature.

The Janus−PNIPAM nanoparticles aggregated and precipitated out of suspension at a pH of 3, because PNIPAM did not provide sufficient steric stabilization of the uncharged nanoparticles at this pH.

Both types of Janus nanoparticles had hydrodynamic diameters of about 10 nm for the individual particles, but self-assembled to form structures with hydrodynamic diameters of 80−90 nm. These sizes suggest that the self-assembled structures formed were elongated, or rod shaped, consistent with the predictions of recent Monte Carlo simulations of our Janus nanoparticles and with cryo-TEM images of these structures.[18] We can estimate the length of the cluster using a cylinder model,[25] according to which a cylindrical self-assembled structure of 20 nm diameter and 170 nm length will have a hydrodynamic diameter of 80 nm. Again, this is consistent with simulations and cryo-TEM images published earlier.

It is interesting to compare the self-assembly behavior of the two types of Janus nanoparticles. With the Janus−PSSNa nanoparticles, the uncharged PAA nanoparticle coating itself is the hydrophobic surface, and the nanoparticles are on the inside of the structure that forms. The Janus−PNIPAM nanoparticles have the opposite structure, that is, the charged PAA-coated nanoparticle surfaces provided cluster stabilization, and the thermally responsive polymer (PNIPAM) is located within the inner regions of the structures.

CONCLUSIONS

We have prepared two types of Janus nanoparticles consisting of ~5 nm magnetite nanoparticles coated on one side with a pH-dependent but temperature-independent polymer (PAA), and functionalized on the other side by a second polymer that is either pH-independent (PSSNa) or temperature-dependent (PNIPAM). The attachment of the polymers to the nanoparticles was confirmed by FTIR and XPS, and their anisotropic structures were evident in TEM images. These Janus nanoparticles can be dispersed individually (~10 nm) at high pH values or low temperature, but can self-assemble at low pH values (Janus−PSSNa particles) or at temperatures greater than 31 °C (Janus−PNIPAM particles). A stable dispersion of clusters of approximately 80−100 nm in diameter can be formed at low pH values or at high temperatures for Janus−PSSNa and Janus−PNIPAM nanoparticles, respectively. These self-assembled structures can be reversed readily by increasing the pH or decreasing the temperature, depending on the type of nanoparticle.

This procedure for the synthesis of stimuli-responsive Janus nanoparticles has significant potential for the guided assembly of nanoparticle structures, as the nature and size of the different polymers used in these systems can be varied to provide, in principle, different desired structural attributes.

METHODS

Materials. Iron tri(acetylacetonate) ($Fe(acac)_3$)(97%), 1,2-tetradecanediol (90%), oleic acid (OA) (90%), oleyl amine (OAm)(70%), benzyl ether (99%), galactaric acid (97%), dimethyl sulfoxide (DMSO) (99.6%), 1-2,dichlorobenzene (DCB) (99%), *N*,*N*′-dimethylformamide (DMF) (99.8%), propionyl bromide (BMPB) (98%), trimethylsilyl acrylate (TMSA) (98%), copper(I) bromide (CuBr) (98%), 1,1,4,7,10,10-hexamethyltriethyltetramine (HMTETA) (97%), 2,2′-azobis (2-methylpropionamidine) dihydrochloride (97%), 4-styrenesulfonic acid sodium salt hydrate (SSNa) (98%), 1-ethyl-3-(3-dimethylaminopropyl) carbodiimide hydrochloride (EDC) (97%), *N*-hydroxysuccinimide (NHS) (98%), tetraethyl orthosilicate (TEOS), and potassium bromide (≥99%, IR grade) were purchased from Sigma Aldrich. Methanol (99.8%), ethylene glycol (98%), acetone (99.5%), isopropanol (99%), and hydrochloric acid (38%) were purchased from Mellinkrod. Hexane (99.9%) was purchased from Omnisolv. Triethylamine (99.9%) and amonium hydroxide (30%) were purchased from J. T. Baker. Sodium hydroxide (NaOH) (99%) was purchased from Mallinckrodt Chemicals. *N*-Trimethoxysilylpropyl-*N*,*N*,*N*-trimethylammonium chloride (TMSPTMAC) (50% in methanol) was purchased from Gelest. Amino terminated poly(*N*-isopropyl acrylamide) (M_n: 50500) was purchased from Polymer Source, Inc. All chemicals were used as received. All water utilized in the experiments was Milli-Q (Millipore) deionized water.

Synthesis. ***Preparation of the Magnetic Nanoparticles.*** The Fe_3O_4 nanopartilces were synthesized using Sun's method.[1,2] $Fe(acac)_3$ (2mmol), 1,2-tetradecanediol (10mmol), oleic acid (6mmol), oleylamine (6mmol), and benzyl ether (20 mL) were mixed under constant flow of nitrogen for 30 min. The solution was heated gradually to 100 °C for an overall period of 45 min. Subsequently, the mixture was heated to 200 °C for 40 min and kept at 200 °C. Finally, under the blanket of nitrogen, the mixture was heated to reflux (~290 °C) for 1 h and then cooled to room temperature. The reaction solution was centrifuged at 7000 rpm for 10 min in an Eppendorf 5810R centrifuge, with 40 mL of methanol. The precipitate was dispersed in 20 mL of hexane and centrifuged again to remove any undispersed residue. The magnetic nanoparticles were precipitated with excess of methanol and separated by means of an electromagnet (Magnetic Separator model L-1; S.G. Frantz Co., Inc.). The particles were dried at 80 °C.

Preparation of Magnetic Nanoparticle Macroinitiators. The magnetic nanoparticles prepared as above (120 mg) and galactaric acid (1.0 g) were mixed in a DCB (7.5 mL) and DMSO (7.5 mL) solvent blend to enable the ligand exchange reaction for replacement of oleic acid and oleyl amine with galactaric acid. The mixture was stirred at 100 °C for 24 h. The particles were precipitated out by adding ethyl ether (40 mL) and recovered by an electromagnet. The magnetic nanoparticles were washed three times with acetone and again recovered electromagnetically. Following drying at 80 °C, the nanoparticles were dispersed in DMF, and 1 mL of triethylamine was added, followed by the dropwise addition of 0.5 mL of 2-bromo-2-methylpropionyl bromide. The acylation reaction that occurred over a period of 3 h at room temperature ensured that Br was present on the surfaces of the magnetic nanoparticles as an initiator for ATRP. These magnetic nanoparticle macroinitiators were washed three times with acetone, recovered by an electromagnet, and then dried at 80 °C.

Preparation of PAA-Coated Core−shell Magnetic Nanoparticles. The magnetic nanoparticle macroinitiators were dispersed in 15 mL of DMSO inside a three-neck round-bottom flask, and 5 mL of TMSA and 0.11 g of CuBr were added to this mixture. Nitrogen was bubbled through this mixture for 30 min under vigorous stirring, following which 0.4 mL of HMTETA was added and the polymerization reaction was allowed to proceed at 50 °C for 48 h. The polymer-coated nanoparticles were recovered by an electromagnet, washed three times with THF to remove free polymer and five times with methanol to remove catalyst, and then redispersed in 40 mL of methanol with sonication for 1 h to remove the protecting TMSA moiety, yielding the desired PAA-coated core−shell magnetic nanoparticles. Fifteen milliliters of water were added to the magnetic nanoparticle dispersions and the mixture pH was increased to 9 by adding 1 N NaOH aqueous solution. The PAA-coated magnetic nanoparticles were filtered magnetically to remove unwanted nanoparticle clusters[6] and then dialyzed against water at pH 9 across a 50 kDa cellulose membrane for 24 h to yield a final dispersion volume of about 30 mL.

Preparation of Silica Beads. A mixture of TEOS (0.35 mol/L), NH_3 (1.16 mol/L), H_2O (3.1 mol/L), and isopropyl alcohol (123 mL) was stirred at 40 °C for 1 h to produce silica beads, which were recovered by centrifugation and washed several times with water under centrifugation. The silica beads were dispersed in concentrated HCl aqueous solution (50 mL, ~6 wt % HCl) and sonicated for 1 h before being centrifuged out and washed several times with water under centrifugation. The beads were dried at 80 °C and then dispersed in a solution of TMSPTMAC (15 mL) in xylene (60 mL); the mixture was heated to reflux at 140 °C (during this process, the methanol released from TMSPTMAC was removed by condensation) and kept at this temperature overnight; the silica beads formed a solid paste-like material in vessel during this process. The liquid was removed, and the silica beads were stored in a vacuum oven for 48 h at 140 °C, washed with water several times under centrifugation, and then dried at 80 °C.

Preparation of PSSNa. SSNa (20 mMol) and 2,2′-azobis(2-methylpropionamidine)dihydrochloride (0.2 mMol) were dissolved in a mixed solvent of ethylene glycol (15 mL) and water (5 mL) under constant flow of nitrogen for 30 min. Then the mixture was heated to 120 °C for 24 h. The polymer was precipitated with excess acetone, dissolved in water, and dialyzed for 48 h against excess water across a 3.5 kDa membrane to remove the residual initiator, and SSNa monomer, and oligomers. The polymer was dried by evaporation. The polymer molecular weight was estimated to be 106 kDa by static light scattering using the Zimm plot method.

Preparation of Janus Nanoparticles. A suspension of 0.2 g of the positively charged silica particles in 10 mL of a 20 mM phosphate-buffered aqueous solution at pH 6 was added gradually under stirring to 10 mL of the PAA-coated magnetic nanoparticle dispersion, and the mixture was stirred for 4 h to allow adsorption of the negatively charged nanoparticles onto the silica beads. The resulting heteroparticles of silica beads and PAA-coated magnetic nanoparticles were centrifuged out, washed three times with water under centrifugation, and then redispersed in 10 mL water, to ensure that there were no free nanoparticles in suspension. The second polymer solution (ether PSSNa or PNIPAM, 5 wt %) and then 0.1 g of NHS and 0.1 g of EDC, were added to the heteroparticle dispersion, and the mixture was stirred for 24 h. The particles were then centrifuged out and again washed three times with water under centrifugation to remove excess polymer and other reagents. Finally 10 mL of water was added to redisperse the heteroparticles. This procedure resulted in only asymmetrical functionalization of the nanoparticles, all of which were adsorbed on the beads; there were no freely suspended nanoparticles that could be evenly coated with the attached polymers.

The Janus nanoparticles were detached from the silica beads by electrostatic repulsion on reversal of the charge on the silica beads following the addition of 0.2 mL of a 1 N NaOH solution. The mixture was stirred for 2 h, following which the large silica beads were removed by centrifugation. The supernatant, which included the Janus nanoparticles, was dialyzed against water across a 50 kDa cellulose membrane.

Measurements. ***Transmission Electron Microscopy (TEM).*** TEM was performed on JEOL 200-CX and 2010 transmission electron micro-

scopes. Samples were prepared by placing drops of the nanoparticle dispersion on lacey carbon-coated 200Mesh copper grids made by Structure Probe Inc. and imaged at an accelerating voltage of 200 kV.

ζ Potential Measurements. All ζ potential measurements were performed using a Brookhaven ZetaPALS ζ potential analyzer (Brookhaven Instruments Corporation). The Smoluchowski equation was used to calculate the ζ potential from the electrophoretic mobility. The reported ζ potential values are an average of 5 measurements, each of which was obtained over 20 electrode cycles. The pH of Janus−PSSNa nanoparticles suspensions was controlled using various buffers: glycine-HCl buffer for pH 10, phosphate buffer (monosodium phosphate, monohydrate plus sodium phosphate, heptahydrate) for pH 8 and pH 6, acetate buffer for pH 5 and pH 4, phosphate buffer (phosphoric acid + monosodium phosphate, monohydrate) for pH 2. Buffer concentration was about 10 mM in the samples. The Janus−NIPAM nanoparticle suspensions were adjusted to pH 9 by adding NaOH aqueous solution.

Dynamic Light Scattering (DLS). DLS experiments were performed using a Brookhaven BI-200SM light scattering system (Brookhaven Instruments Corporation) at an angle of 90°. The Contin program was used for hydrodynamic diameter determinations from the DLS correlation functions. Samples were measured for 3 min, and the reported diameters are the average of three repeated measurements. The pH of each sample was the same as that used in the ζ potential measurements.

Fourier Transform Infrared Spectroscopy (FTIR). FTIR spectroscopy was performed on a NEXUS 870 FTIR spectrometer (Thermo Nicolet Inc.). Spectra were recorded over the wavenumber range between 4000 and 400 cm^{-1} at a resolution of 2 cm^{-1} and are reported as the average of 64 spectral scans. All samples were dried overnight at 80 °C in a vacuum oven and then ground and mixed with KBr to form the pellets used in the measurements.

X-ray Photoelectron Spectrometry (XPS). XPS was carried out on a Kratos AXIS Ultra Imaging X-ray photoelectron spectrometer with monochromatized Al Ka radiation at 1486.69 eV and with steps of 1000 meV for 50 ms. Each sample was dialyzed against water for 48 h and subsequently freeze-dried.

Acknowledgment. The assistance of Yong Zhang in the performance of the high resolution TEM and the assistance of Elisabeth L. Shaw for the XPS are gratefully acknowledged. We also gratefully acknowledge the many fruitful discussions with Lev Bromberg on polymer selection. This work was supported by the Mitsubishi Chemical Corporation.

REFERENCES AND NOTES

1. Sun, S.; Zeng, H. Size-Controlled Synthesis of Magnetite Nanoparticles. *J. Am. Chem. Soc.* **2002**, *124*, 8204–8205.
2. Sun, S.; Zeng, H.; Robin, D. B.; Raoux, S.; Rice, P. M.; Wang, S. X.; Li, G. Monodisperse MFe_2O_4 (M = Fe, Co, Mn) Nanoparticles. *J. Am. Chem. Soc.* **2004**, *126*, 273–279.
3. Wang, L. Y.; Luo, J.; Fan, Q.; Suzuki, M.; Suzuki, I. S.; Engelhard, M. H.; Lin, Y.; Kim, N.; Wang, J. Q.; Zhong, C. J. Monodispersed Core-Shell Fe_3O_4@Au Nanoparticles. *J. Phys. Chem. B* **2005**, *109*, 21593–21601.
4. Cho, S. J.; Idrobo, J. C.; Olamit, J.; Liu, K.; Browning, N. D.; Kauzlarich, S. M. Growth Mechanisms and Oxidation Resistance of Gold-Coated Iron Nanoparticles. *Chem. Mater.* **2005**, *17*, 3181–3186.
5. Mikhaylova, M.; Kim, D. K.; Bobrysheva, N.; Osmolowsky, M.; Semenov, V.; Tsakalakos, T.; Muhammed, M. Superparamagnetism of Magnetite Nanoparticles: Dependence on Surface Modification. *Langmuir* **2004**, *20*, 2472–2477.
6. Lattuada, M.; Hatton, T. A. Functionalization of Monodisperse Magnetic Nanoparticles. *Langmuir* **2007**, *23*, 2158–2168.
7. White, M. A.; Johnson, J. A.; Koberstein, J. T.; Turro, N. J. Towards the Syntheses of Universal Ligands for Metal Oxide Surfaces: Controlling Surface Functionality through Click Chemistry. *J. Am. Chem. Soc.* **2006**, *128*, 11356–11357.
8. Shamim, N.; Hong, L.; Hidajat, K.; Uddin, M. S. Thermosensitive Polymer (*N*-isopropylacrylamide) Coated Nanomagnetic Particles: Preparation and Characterization. *Colloids Surf. B* **2007**, *55*, 51–58.
9. Gravano, S. M.; Dumas, R.; Liu, K.; Patten, T. E. Methods for the Surface Functionalization of γ-Fe_2O_3 Nanoparticles with Initiators for Atom Transfer Radical Polymerization and the Formation of Core-Shell Inorganic-Polymer Structures. *J. Polym. Sci., Part A* **2005**, *43*, 3675–3688.
10. Kalsin, A. M.; Fialkowski, M.; Paszewski, M.; Smoukov, S. K.; Bishop, K. J. M.; Grzybowski, B. A. Electrostatic Self-Assembly of Binary Nanoparticle Crystals with a Diamond-Like Lattice. *Science* **2006**, *312*, 420–424.
11. Klajn, R.; Bishop, K. J. M.; Fialkowski, M.; Paszewski, M.; Campbell, C. J.; Gray, T. P.; Grzybowski, B. A. Plastic and Moldable Metals by Self-Assembly of Sticky Nanoparticle Aggregates. *Science* **2007**, *316*, 261–264.
12. Ge, J.; Hu, Y.; Biasini, M.; Beyermann, W. P.; Yin, Y. Superparamagnetic Magnetite Colloidal Nanocrystal Clusters. *Angew. Chem., Int. Ed.* **2007**, *46*, 4342–4345.
13. Ge, J.; Hu, Y.; Yin, Y. Highly Tunable Superparamagnetic Colloidal Photonic Crystals. *Angew. Chem., Int. Ed.* **2007**, *46*, 7428–7431.
14. Perro, A.; Reculusa, S.; Ravaine, S.; Bourgeat-Lami, E.; Duguet, E. Design and Synthesis of Janus Micro- and Nanoparticles. *J. Mater. Chem.* **2005**, *15*, 3745–3760.
15. Pradhan, S.; Xu, L. P.; Chen, S. Janus Nanoparticles by Interfacial Engineering. *Adv. Funct. Mater.* **2007**, *17*, 2385–2392.
16. Xu, L. P.; Pradhan, S.; Chen, S. Adhesion Force Studies of Janus Nanoparticles. *Langmuir* **2007**, *23*, 8544–8548.
17. Gu, H.; Yang, Z.; Gao, J.; Chang, C. K.; Xu, B. Heterodimers of Nanoparticles: Formation at a Liquid−Liquid Interface and Particle-Specific Surface Modification by Functional Molecules. *J. Am. Chem. Soc.* **2005**, *127*, 34–35.
18. Lattuada, M.; Hatton, T. A. Preparation and Controlled Self-Assembly of Janus Magnetic Nanoparticles. *J. Am. Chem. Soc.* **2007**, *129*, 12878–12889.
19. Schild, H. G. Poly(*N*-isopropylacrylamide): Experiment, Theory and Application. *Prog. Polym. Sci.* **1992**, *17*, 163–249.
20. Teodorescu, M.; Matyjaszewski, K. Atom Transfer Radical Polymerization of (Meth)acrylamides. *Macromolecules* **1999**, *32*, 4826–4831.
21. Hsu, W. P.; Yu, R.; Matijevi, E. Paper Whiteners I. Titania Coated Silica. *J. Colloid Interface Sci.* **1993**, *156*, 56–65.
22. Stöber, W.; Fink, A.; Bohn, E. Controlled Growth of Monodisperse Silica Spheres in the Micron Size Range. *J. Colloid Interface Sci.* **1968**, *26*, 62–69.
23. Landim, A. S.; Filho, G. R.; Assunção, R. M. N. Use of Polystyrene Sulfonate Produced from Waste Plastic Cups as an Auxiliary Agent of Coagulation, Flocculation and Flotation for Water and Wastewater Treatment in Municipal Department of Water and Wastewater in Uberlândia-MG, Brazil. *Polym. Bull.* **2007**, *58*, 457–463.
24. Bourlinos, A. B.; Bakandritsos, A.; Georgakilas, V.; Petridis, D. Surface Modification of Ultrafine Magnetic Iron Oxide Particles. *Chem. Mater.* **2002**, *14*, 3226–3228.
25. Schmitz, K. S. *Dynamic Light Scattering by Macromolecules*; Academic Press: New York, 1990.